

Penetration of the non-migrating atmospheric diurnal tide into polar latitudes

Takehiko Aso

*Arctic Environment Research Center, National Institute of Polar Research,
Kaga 1-chome, Itabashi-ku, Tokyo 173-8515*

Abstract: Classical theory of atmospheric tide predicts the confinement of propagating diurnal tide to lower latitudes equatorward of 30° latitude for which diurnal frequency exceeds the local Coriolis frequency. Observations so far averaged over appropriate periods, however, suggest the pervasion of propagating tide at meteor heights especially in wintertime in view of vertical phase structure. These might possibly be interpreted by the numerical modeling as the penetration of non-migrating higher zonal wave number tides which can be propagating in the counter-stream Doppler effect of the background mean zonal wind.

1. Introduction

The atmospheric tide is a global-scale wave system which is of standing nature with respect to latitude and propagates only in the zonal and altitude directions (*e.g.*, Chapman and Lindzen, 1970). When a tidal disturbance is excited locally, it will propagate both in latitudinal and longitudinal directions as well as in the vertical direction. After it spreads over in the horizontal plane, an organized wave structure is eventually attained with relevant Hough functions diminishing at the poles so that it has finite velocity at the poles and with the periodic condition satisfied in the zonal direction. This describes transient response to disturbances by localized forcing like Joule or Lorentz couplings at higher latitudes. Between the paradigm of a transient development of tidal perturbation and a globally organized tidal mode, complications exist, to be resolved through available mechanistic tidal modeling.

In this paper, a description is given on the characteristics of the diurnal tide at polar latitudes where Hough functions and associated velocity expansion functions take particular values. Some typical results evidenced for meteor heights of 80–100 km are briefly reviewed, especially in view of its propagating and evanescent behaviors.

When we consider diurnal perturbation, it is anticipated that the diurnal tide is, by and large, evanescent with respect to altitude poleward of 30° latitude in that the Coriolis frequency $2\omega \cos\theta$ exceeds the diurnal frequency ω (θ : colatitude, ω : earth rotation rate $7.292 \times 10^{-5} \text{ s}^{-1}$).

Numerical modeling of diurnal tides are then compared with these facts in which the non-migrating tide as well as the migrating component have been calculated using a steady and viscid model with background mean zonal wind and latitudinal temperature gradient. A suggestion will be given for future planned collaborative observation along

longitudinal and latitudinal chains to clarify tidal modes which play a dominant role at polar latitudes.

2. Observational evidences

Tidal studies with radars at high latitudes have long been relatively scarce compared to mid to low latitudes since we first participated in the global campaign in late 1970's by the Kyoto meteor radar (Aso *et al.*, 1979). But more recently, efforts are focused also on polar latitudes where various interesting phenomena around the geophysically singular point are taking place in relation to *in-situ* excitation by the energy input from solar wind and the magnetosphere and to dynamical coupling from the lower atmosphere pervaded by the polar vortex.

In 1985, the auroral radar at Syowa, Antarctica (69°S) was occasionally operated in a meteor trail detection mode (Ogawa *et al.*, 1985). Based on these wind data, altitude profile of diurnal tide is analyzed for equinoctial and solstitial months as shown in Fig. 1. In the figure, northward wind at equinox shows its phase (local time at its maximum) around 2400 LT for three *K*-index classifications of the geomagnetic disturbances, though it has some variances. In June solstice, however, phase shows downward progression with inferred vertical wavelength of about 80 km. A height is determined by the conventional decay-height method with height uncertainty of several km, but this tends to average out the phase excursion, so the data suggest that the detected diurnal tide is a

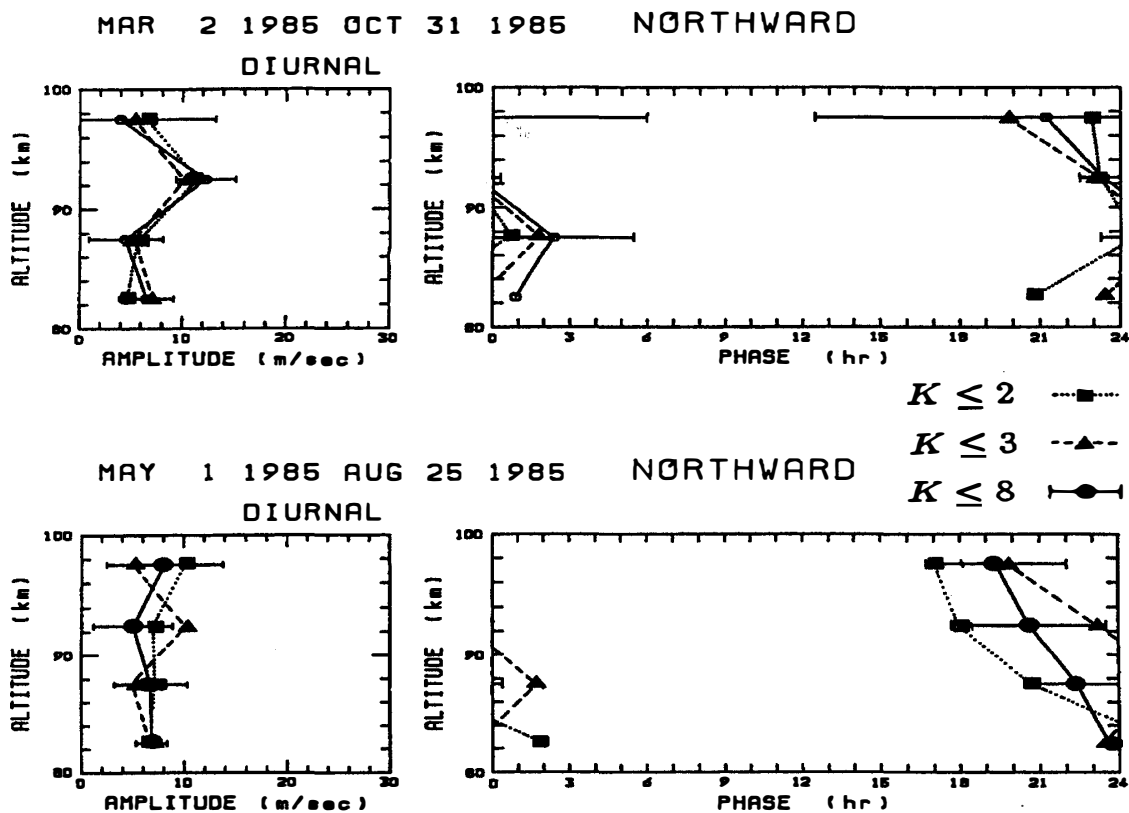


Fig. 1. Amplitude and phase of the diurnal component of the meridional wind observed at Syowa during equinoctial (top) and June solstitial (bottom) months in 1985. See the text for details.

mixture of evanescent and propagating modes in this winter observation. A geomagnetic disturbance effect on tide is still open to question and will be discussed elsewhere.

Figure 6 of Manson *et al.* (1991) also shows the 6-days averages of the diurnal tide in December observed by Tromsø MF radar at 70°N. In the figure, the phase gradient suggests the propagating nature with vertical wavelength of about 30 km, much shorter than in Fig. 1.

With regard to earlier observations, Carter and Balsley (1982) shows the summer averaged result of diurnal tide at Poker Flat (65°N) in which eastward phase lies between 1800–2000 LT and northward phase around 1200–1600 LT below 88 km with slight phase lag at higher altitudes. The result of constant phase values is consistent with theoretical prediction referred to in the next section. Avery *et al.* (1989) summarized the observed results of tides at higher latitudes. They found almost evanescent nature during non-winter time and strong phase gradient in winter, suggesting *in-situ* forcing or mode superposition occurring at these heights. These results are replotted and compared in Fig. 2. In addition, Fig. 4b of Nozawa and Brekke (1999) illustrates tidal-period component analysis for the *E* region neutral wind over 56 days observed by the EISCAT radar, in which the diurnal phase in winter shows irregular variation with altitude while in summer or equinox it is almost constant around 1000–1200 LT at its northward maximum. Also, Murayama *et al.* (1999) reported the seasonal variation of diurnal tide observed by their MF radar facility at Poker Flat, Alaska, which shows that the northward phase is rather erratic in wintertime than in other seasons. Our result in Fig. 1 at Syowa as well as Fig. 2 and other findings suggest that in wintertime the phase indicates somewhat propagating characteristic whereas it is, by and large, evanescent in other seasons. We must also add that positive phase gradient is also possible in the mixture of evanescent and propagating

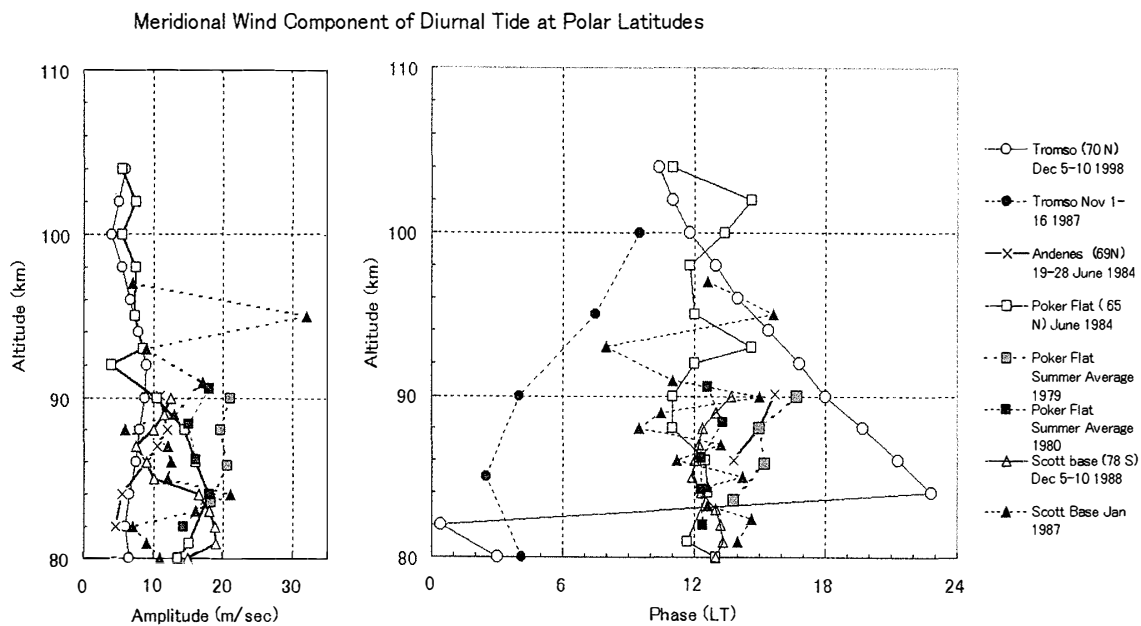


Fig. 2. Summarized plots of the observed meridional component of the diurnal tide at polar latitudes. Amplitudes and phase values are taken from Avery *et al.* (1989), Manson *et al.* (1991) and Carter and Balsley (1982). Phase values in the Southern Hemisphere are shifted by 12 hrs to compare with the Northern Hemisphere.

modes in the phasor diagram even in case of no *in-situ* forcing above these heights as shown later in Fig. 3.

3. Theoretical prediction

In the conventional classical tidal calculation, propagating (1, 1) mode is very small poleward of 60° latitude whereas evanescent (1, -2) mode is dominant at higher latitudes though it tends to decrease above assumed forcing layer in the lower atmosphere. Combined (1, 1) plus (1, -2) forcing indicates wind fields at 75° latitude are evanescent up to 100 km with eastward and northward phase of 1800 LT and 1200 LT, respectively. Northward phase of about 2400 LT at Syowa in equinoctial months and observational results by Carter and Balsley (1982) and Fraser *et al.* (1995) are both fairly consistent.

A viscid modeling called ATM2 (Atmospheric Tidal Modeling Ver. 2) of diurnal tide has been performed to estimate the effect of background mean zonal wind and vertical diffusion (Aso *et al.*, 1987). The formulation comprises coupled partial differential equations for the velocity vector and temperature perturbations. After discretization in latitude, the Lindzen and Kuo algorithm (Lindzen and Kuo, 1969) is used for the ordinary differential equation in altitude with appropriate boundary conditions. This model circumvents the apparent singularity for the diurnal tidal calculation at θ (colatitude) = 60° which is encountered in the inviscid model with background zonal wind and simpler dissipation of parameterized Rayleigh friction and Newtonian cooling (Lindzen and Hong, 1974; Aso *et al.*, 1981).

Viscid modeling suggests that ozone forcing shows dominant (1, -2) evanescent mode at 75°N up to 110 km, while water vapor of smaller vertical extent excites less dominant propagating component there, the overall characteristic being indicative of evanescent mode poleward of 60°N latitude. It must be added that *in-situ* forcing is not included in the model.

Figure 3a shows the northerly wind component of diurnal tide at various northern latitudes for December solstice conditions. The grid size is 2.5° in latitude and 250 m in altitude from 0 to 150 km region. It is clearly seen that at poleward of 60°N, the amplitude is smaller at meteor heights and evanescent modes are dominant with northerly phase at 0000 LT and westerly phase leading by 90° in the northern hemisphere. This is of course consistent with the southern hemisphere northward maximum at 0000 LT as mentioned before.

In this calculation, both horizontal diffusion and gravity wave drag which is parameterized as an effective Rayleigh friction (Forbes *et al.*, 1991) are also included. Tidal climatology modeling assuming mean zonal wind and temperature based on the monthly model of CIRA 86 has been used in this model. The result shown in Fig. 3b is that at 75°N latitude, the amplitude of the horizontal wind varies by several factors but the phase change is less than 1 hour at 80–100 km altitude region.

The theoretical prediction by Forbes and Hagan (1988) based on the similar viscid model also illustrates an almost evanescent diurnal tide at 70°N with eastward and northward phase of 1800 LT and 1200 LT, respectively.

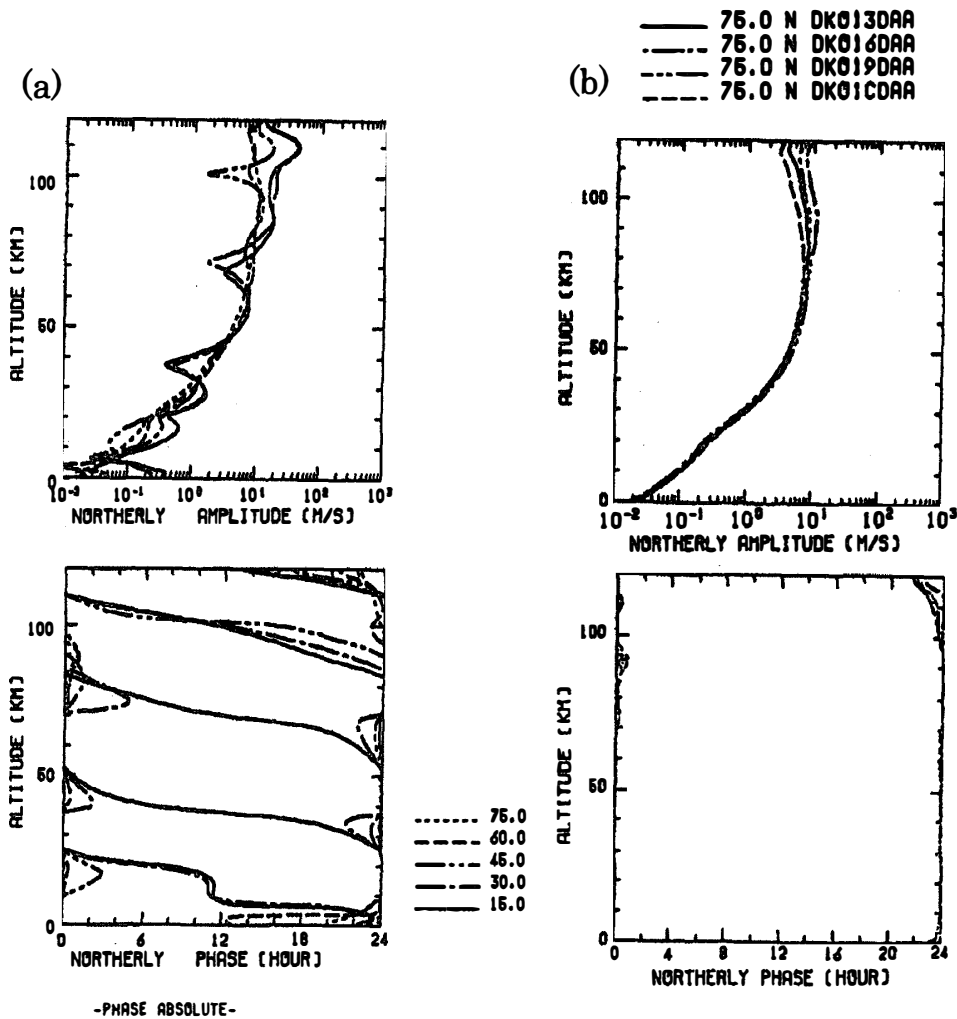


Fig. 3. Amplitude and phase of the meridional component of viscid-model diurnal tide versus height (a) for December wind and forcing conditions at latitudes of 15°(solid), 30°(dashed-dot), 45°(dashed-double-dot), 60°(dashed), and 75°(dotted) in the Northern Hemisphere, and (b) for monthly mean background wind model of March (solid), June (dashed-dot), September (dashed-double-dot), and December (dashed) at 75°N latitude.

4. Penetration of non-migrating tide

The viscid model used for the modeling of tidal climatology as in Fig. 3 is now applied to non-migrating tidal regime by assuming differential heat transferred only from the ground as a localized, non-migrating heating source. In the present calculation, Fourier components relevant to particular zonal wavenumbers are used as a forcing agent. The vertical structure is an exponential decrease with an e-fold thickness of 1 km. More quantitatively, longitudinally varying heating due to global distribution of ozone and water vapor insolation absorption, latent heat release in the boundary layer, dry convection heating and eddy thermal conduction heating are the refinements to these as possible candidates for exciting non-migrating tides (Ekanayake *et al.*, 1997).

Contour plots of the latitudinal structures of northerly wind amplitude and phase for the westward propagating non-migrating diurnal tide with zonal wave number $s = 6$ are

shown in Fig. 4. In this calculation, the background mean zonal wind at June solstice is assumed which is based on CIRA 72 model. Hence in the southern hemisphere where the winter westerly wind dominates at stratosphere and mesosphere heights, the amplitude tends to be larger at higher latitudes, maximizing at around 85 km and 50°S. A possible explanation is the following. A momentum conservation equation for tidal perturbations in the atmosphere with background westerly wind V has a term $\partial/\partial t + V/a \sin\theta \partial/\partial\phi$ which leads to a Doppler shifted wave frequency of $\tilde{\sigma} = \sigma + sV/a \sin\theta$ for wave frequency σ and zonal wave number s , positive for westward and negative for eastward propagation. In the westerly wind regime, the $s=6$ westward propagating mode as in Fig. 4 has a higher frequency than the local Coriolis frequency, thus a vertically propagating wave can permeate up to higher latitudes. The background zonal wind in the southern hemisphere is a strong westerly greater than 60 m/s at around 50°S. A Doppler-shifted wave frequency for $s=6$ is about 2.2ω which exceeds $f=1.5\omega$ at this latitude. These findings are also consistent with the suggestion on non-migrating tides envisaged in the General Circulation Model simulation by Miyahara *et al.* (1993)

The phase diagram also indicates a short vertical wavelength of 15 km at around the 80 km and 60°S region. The vertical wavelength of this component for an isothermal, stationary atmosphere with a temperature of 260 K is 17, 13, and 10 km for (1, 6, 1), (1, 6, 2) and (1, 6, 3) modes with equivalent depths of 0.292, 0.158 and 0.097 km, respectively. These values are consistent with the inferred short wavelength characteristic

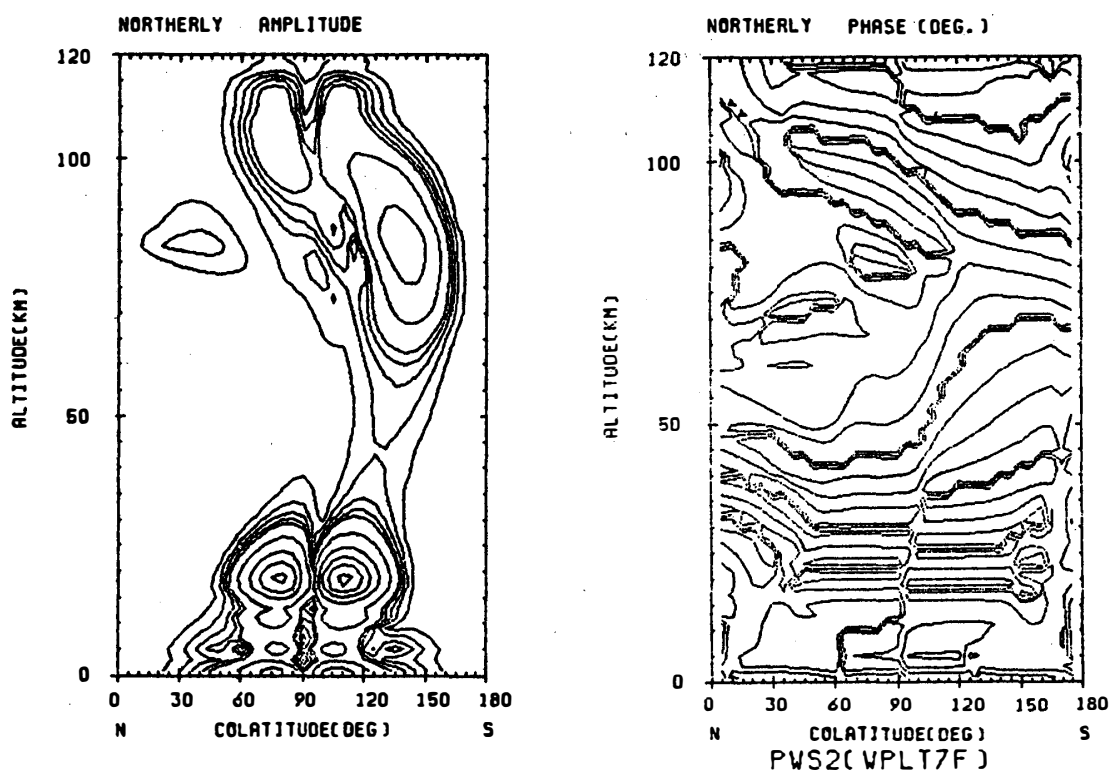


Fig. 4. Contour plots of the latitudinal structures of amplitude and phase of northerly velocity component for the viscous model diurnal non-migrating tide with zonal wavenumber $s=6$. Contour intervals are 1, 0.8, 0.6, 0.4, 0.2 times the power of 10 in amplitude and 0, $\pm 90^\circ$ and $\pm 180^\circ$ in phase.

in Fig. 4. It must be recalled, however, that a simple modal concept no longer holds for latitudinally varying temperature and mean wind regime.

Henceforth, we should continue to study if this is the case or other agents, say, *in-situ* or auroral excitations are complicating an apparent 24 hr-period component.

5. Summary and conclusion

This paper emphasizes the existence of a vertically propagating diurnal component in the polar mesopause regions mostly in wintertime where evanescent modes are supposed to dominate based upon classical tidal theory. Meteor and MF radar observations at Antarctica and Tromsø reported well-defined signatures of downward phase progression or phase excursion indicative of a superposition of propagating modes on a constant-phase evanescent component at these heights.

One possible interpretation is suggested here by a numerical viscous model of atmospheric tides which assumes a background mean zonal flow and realistic dissipative processes including eddy and molecular diffusivity. It is found that the non-migrating tide excited by a differential heat flux from land-sea contrast tends to penetrate to the hemisphere with a background wind opposite to its longitudinal propagation direction, and a Doppler-shifted frequency exceeding local Coriolis frequencies.

Zonally coordinated observations which resolve the zonal wavenumber of involved 24 hr oscillations are requisite to gainsay the conjectures of possible agents for no local solar forcing in winter, *e.g.*, an *in-situ* forced pseudotide like 24 hr oscillation via gravity wave momentum flux modulation or auroral disturbances and also various non-linear interactions taking place in the whole mesosphere regions. To this end, an international coordination is now planned, aiming at both the conjunctive MF/meteor/MST/HF/EISCAT radar operation in the Arctic region and a conjugate comparison with an Antarctic MF radar network.

Acknowledgments

The author thanks anonymous referees for their kind comments and suggestions in reviewing the paper.

The editor thanks Drs. Saburo Miyahara and Grahame Fraser for their help in evaluating this paper.

References

- Aso, T., Tsuda T. and Kato, S. (1979): Meteor radar observations at Kyoto University. *J. Atmos. Terr. Phys.*, **41**, 517–525.
- Aso, T., Nonoyama, T. and Kato, S. (1981): Numerical simulation of semidiurnal atmospheric tides. *J. Geophys. Res.*, **86**, 11388–11400.
- Aso, T., Ito, S. and Kato, S. (1987): Background wind effect on the diurnal tide in the middle atmosphere. *J. Geomagn. Geoelectr.*, **39**, 297–305.
- Avery, S., Vincent, R.A., Phillips, A., Manson, A.H. and Fraser, G.J. (1989): High-latitude tidal behavior in the mesosphere and lower thermosphere. *J. Atmos. Terr. Phys.*, **51**, 595–608.
- Carter, D.A. and Balsley, B.B. (1982): The summer wind field between 80 and 93 km observed by the

- MST radar at Poker Flat, Alaska (65°N). *J. Atmos. Sci.*, **39**, 2905–2915.
- Chapman, S. and Lindzen, R.S. (1970): *Atmospheric Tides*. Dordrecht, D. Reidel.
- CIRA86 (1990): *COSPAR International Reference Atmosphere: 1986, Part II*, ed. by D. Rees. Oxford, Pergamon Press.
- Ekanayake, E.M.P., Aso, T. and Miyahara, S. (1997): Background wind effect on propagation of nonmigrating diurnal tides in the middle atmosphere. *J. Atmos. Solar-Terr. Phys.*, **59**, 401–429.
- Forbes, J.M. and Hagan, M.E. (1988): Diurnal propagating tide in the presence of mean winds and dissipation: A numerical investigation. *Planet. Space Sci.*, **36**, 579–590.
- Forbes, J.M., Gu, J. and Miyahara, S. (1991): On the interactions between gravity waves and the diurnal propagating tide. *Planet. Space Sci.*, **39**, 1249–1257.
- Fraser, G.J., Portnyagin, Y.I., Forbes, J.M., Vincent, R.A., Lysenko I.A. and Makarov, N.A. (1995): Diurnal tide in the antarctic and arctic mesosphere/lower thermosphere regions. *J. Atmos. Terr. Phys.*, **57**, 383–393.
- Lindzen, R.S. and Hong, S.-S. (1974): Effects of mean winds and horizontal temperature gradients on solar and lunar semidiurnal tides in the atmosphere. *J. Atmos. Sci.*, **31**, 1421–1446.
- Lindzen, R.S. and Kuo, H.-L. (1969): A reliable method for the numerical integration of a large class of ordinary and partial differential equations. *Mon. Weather Rev.*, **97**, 732–734.
- Manson, A.H., Meek, C.E., Avery, S.K., Fraser, G.J., Vincent, R.A., Philipps, A., Clark, R.R., Schminder, R., Kurschner, D. and Kazimirovsky, E.S. (1991): Tidal winds from the mesosphere, lower thermosphere global radar network during the second LTCS campaign 1988. *J. Geophys. Res.*, **96**, 1117–1127.
- Miyahara, S., Yoshida, Y. and Miyoshi, Y. (1993): Dynamic coupling between the lower and upper atmosphere by tides and gravity waves. *J. Atmos. Terr. Phys.*, **55**, 1039–1053.
- Murayama, Y., Kato, K., Igarashi, K. and Mori, H. (1999): Variability of 1- and 1/2- day period wind oscillations observed with MF radar at Poker Flat, Alaska. Presented at the 106th SGPSS Meeting in Sendai, Japan, November 1999.
- Nozawa, S. and Brekke, A. (1999): Studies of the auroral *E* region neutral wind through a solar cycle: Quiet days. *J. Geophys. Res.*, **104**, 45–66.
- Ogawa, T., Igarashi, K., Kuratani, Y., Fujii, R. and Hirasawa, T. (1985): Some initial results of 50 MHz meteor radar observation at Syowa Station. *Mem. Natl Inst. Polar Res., Spec. Issue*, **36**, 254–263.

(Received January 12, 2000; Revised manuscript accepted March 14, 2000)